Interface Polymerization in a Polymer Micelle: An NMR Study of the Radical Polymerization of Methyl Methacrylate at the Core−Shell Interface of Polystyrene-*block*-poly(methacrylic acid) Micelles

J. Kříž,* D. Kurková, P. Kadlec, Z. Tuzar, and J. Pleštil

Institute of Macromolecular Chemistry, Academy of Sciences of the Czech Republic, Heyrovsky Sq.2, 162 06 Prague 6, Czech Republic

Received August 12, 1999; Revised Manuscript Received December 27, 1999

ABSTRACT: Systems containing poly(styrene)-*block*-poly(methacrylic acid) micelles (1.67 g/L), methyl methacrylate (1.88−3.76 g/L), and initiator (polymerization) or inhibitor (pure solubilization) in D_2O buffer solution were studied by ^1H NMR. The proton NMR signals of MMA dissolved in the micellar system have the same chemical shifts as those in the corresponding D_2O buffer solution but exhibit a characteristically broadened and asymmetric shape. Separate signals with different chemical shifts and signal shapes were observed for MMA absorbed into the poly(styrene) core. From the shape analysis of the signals of the water-dissolved MMA in the micellar system, it can be deduced that the monomer is almost exclusively accumulated near the core−shell interface. Its radial distribution can be approximated by a Gaussian function with the maximum at the core radius R and half-width b of $1.65R$ and $1.93R$ for the MMA concentrations 2 and 4 g/L, respectively. An increase in temperature from 295 to 330 K leads to a faster self-diffusion of MMA but not to an appreciable broadening of the distribution. When initiated with ammonium peroxysulfate (330 K) or its mixture with potassium disulfite (295 K), MMA at the interface undergoes polymerization. At elevated temperatures such as 330 K, a part of MMA diffuses into the outer layers of the polystyrene core and does not polymerize there, in particular at higher MMA concentrations, being shielded by the peel of PMMA from the initiator radicals. At 295 K, the diffusion is very slow so that no detectable amount of MMA avoids polymerization. The observed polymerization kinetics as well as the MMA signal shape evolution indicate that (i) during polymerization, the PMMA formed diffuses into the vicinity of the core−shell interface and (ii) termination is markedly suppressed in analogy with a gel effect. Mathematical models of the NMR signal shape as well as of diffusion-affected polymerization kinetics under general radial monomer distribution in a micelle are presented and the numerical computer simulations are compared with the experimental data. The results of this study agree with the separately published SANS results in the conclusion that micelles with cores sheeted with multiple layers of different polymers can be prepared by the relatively simple technique presented.

Introduction

Micelles of amphiphilic block copolymers have been studied for quite a long time[1−6] not only as interesting physical systems formed by spontaneous molecular self-assembly but also as potential carriers of active substances such as medical drugs, disinfectants, and others. In the latter respect, the outstanding ability of the hydrophobic micellar core to solubilize many almost water-insoluble substances has been observed,[7] leading thus to the idea of possible controlled uptake and release of such substances in water-based systems. When studying the dynamics of material exchange between the core and the surrounding medium,[9] we have observed a rather swift diffusion of many solubilizates in both directions. This could be a serious obstacle of tailoring the solubilization dynamics to the desired controlled uptake or release. In another study, we have shown[10] that three-layer micelles can be prepared from ABC triblock amphiphilic copolymers, C being a hydrophilic block and A and B mutually incompatible hydrophobic blocks. In such case, block A is resident in the inner part of the core and B forms the core−shell interface. It has been demonstrated that the kinetics of solubilization can be specifically modified by the chemical nature of the block B without impairing seriously the solubilization capacity of the micelle.[10] At the present state of art, preparing the tailored triblock and, potentially, multiblock copolymers could be difficult. Hence, other ways of preparing multilayered micellar cores were sought. One of them is the preparation of onion-like micelles by coprecipitation of suitable block copolymers,[11,12] the polymerization of a suitable monomer in a micelle being another one. In a recent paper,[13] radiation polymerization of 2-ethylhexyl acrylate swelled into the core of poly(2-ethylhexyl acrylate)-*block*-poly(acrylic acid) micelles has been demonstrated. Much earlier, however, a peroxysulfate-initiated polymerization of pyrrole in polystyrene-*block*-poly(methacrylic acid) has been successfully performed.[14] We thus tried the same approach to the system polystyrene-*block*-poly(methacrylic acid) with monomer methyl methacrylate, expecting at least partial segregation of the formed poly(methyl methacrylate) due to its restricted compatibility with poly(styrene). In the SANS study[15] of the polymerization process and the final product, strong evidence of the PMMA onion-like segregation at the core−shell interface has been obtained. According to SANS, this result is due to the monomer residing and polymerizing mostly outside the micellar core rather than to segregation of PMMA formed in the core. This interesting phenomenon calls for a complementary study using an independent method, namely NMR.

* To whom correspondence should be addressed. Tel: 420-2-20403382. Fax: 420-2-367981. E-mail: kriz@imc.cas.cz.

10.1021/ma991368n CCC: $19.00
Published on Web 03/01/2000

Theory

Signal Shape of the Solute Near a Micellar Core. As recognized many years ago,[16,17] a homogeneous spherical object with a magnetic susceptibility χ_1 in a magnetic field $\mathbf{B}_0$ immersed into a homogeneous medium with a different susceptibility χ_2 acts like a magnetic dipole μ inducing thus in its surroundings an additional magnetic field $B(\theta,r)$ of the magnitude

$$B(\theta,r) = \mu(3\cos^2\theta - 1)/r^3 \qquad (1)$$

where θ is the angle of the radius vector of the given point with the axis of the magnetic field $\mathbf{H}_0$ and r is its length. The magnitude of the dipole moment is $\mu = (4/3)\pi R^3(\chi_1 - \chi_2)\mathbf{B}_0$, R being the radius of the spherical object. In conformity with Doskočilová et al.,[17] we shall introduce the constant $A = (4/3)\pi(\chi_1 - \chi_2)\mathbf{B}_0$ and the reduced radius $r' = r/R$. Hence, $B(\theta,r') = A(3\cos^2\theta - 1)/r'^3$. In our first approach, outlined in principle in our recent article,[13] we shall treat the micellar core as a spherical object and the surrounding medium of the hydrated micellar shell as a quasi-continuum of a uniform magnetic susceptibility. This is certainly an approximation, which has to be refined later. Suppose now that the solute molecules are dispersed around the micellar core with a spherically symmetric distribution $g_N(r) = \xi g(r)$, $g(r)$ being an appropriate radial function and ξ a normalization factor

$$\xi = 2(r_{max}{}^3 - R^3)c_0[\int_R^{r_{max}} r^2 g(r)\,dr]^{-1} \qquad (2)$$

The radially dependent angular distribution is $g_N(r,\theta) = (1/2)\sin\theta\, g_N(r)$ and its volume form is $G_N(r,\theta) = 4\pi r^2 g_N(r,\theta)$. Let us assume now that a nucleus at the point (r,θ) has a Lorentzian signal symmetric about the point $\nu(r,\theta) = \nu_0 + \gamma A(3\cos^{2\theta} - 1)R^3/(2\pi r^3)$, where ν_0 is the "natural" shift of the nucleus in the magnetic field $\mathbf{B}_0$ and γ is its gyromagnetic ratio. The shape of the collective signal of nuclei surrounding the spherical core is then

$$I = I_0\int_R^{r_{max}}\int_0^{\pi} G_N(r,\theta)w/\{w^2 + [\nu(r,\theta) - \nu]^2\}\,d\theta\,dr \qquad (3)$$

where the integrand is a weighted Lorentzian with the center at $\nu(r,\theta)$, ν varies from $-\infty$ to $+\infty$, and w is the natural width of the signal in a homogeneous medium. The signal shape clearly depends on A, i.e., on $(\chi_1 - \chi_2)$, R and $G_N(r,\theta)$, hence on the radial distribution $g(r)$.

$$g(r') = \xi/[b(\pi/2)^{1/2}]\exp[-2(r' - 1)^2/b^2] \qquad (4)$$

We have used the Gaussian distribution where b has the usual meaning of the distribution width. We do not insist the functional form in eq 4 has an exact physical meaning. However, it reflects two important features of the probable actual distribution: its statistical nature and the tendency of the solute to accumulate around the micellar core. Figure 1 shows the signal shapes simulated for the Gaussian distribution (b varying from 1.0 to 5.0) using eqs 1−4 with the natural signal width $w = 3$ Hz and A equivalent to 50 Hz. As seen from this example, the more dense population of the solute in the vicinity of the core leads to a broader and more asymmetric signal. It should be noted marginally that the signal of a solute placed *inside* the core is not affected by the magnetic field inhomogeneity, its width being given solely by the dynamic properties of the core medium.

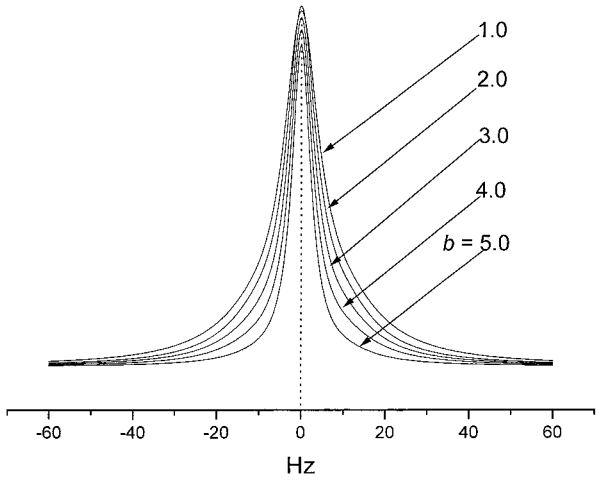

Figure 1. NMR signal shapes simulated for an induced field inhomogeneity (maximum 50 Hz) and a Gaussian distribution of the measured molecules with a different second moment b (natural signal width 3 Hz).

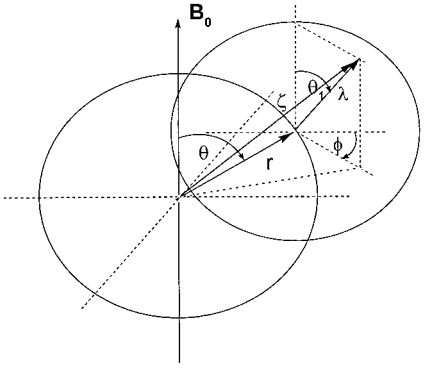

Figure 2. Geometry in the vicinity of the core in the considered case of self-diffusion.

So far, we have implicitly assumed a static position of the given nucleus. As already indicated by Doskočilová et al.,[17] fast diffusion of the solute can change the situation: within the time window of NMR resolution, the molecule can jump to different positions and face different intensities of the local magnetic field. As the exact description of the corresponding effect on the signal shape is rather complicated, we prefer to use the following approximation. The key idea of it consists of the time window or critical time τ given by the maximum broadening Δ, $\tau = {}^1/_2\pi\Delta\nu_{1/2}$. During this time, the molecule traverses a mean distance λ given by the expression $\lambda = (2D\tau)^{1/2} = (D/\pi\Delta\nu_{1/2})^{1/2}$, where D is the diffusion coefficient given by the Einstein−Stokes formula $D = kT/(6\pi\eta\rho)$. As all directions are in principle equivalent, we can imagine that the points the molecule can reach in time τ from the point $\boldsymbol{r}(r,\theta)$ form a sphere with the center in $\boldsymbol{r}$ and the radius λ. At any point of this sphere given by $\boldsymbol{r}$ and the angles θ_1, φ as illustrated in Figure 2, the nucleus is faced by the local field $B(\theta_1,\zeta) = A(3\cos^2\theta_1 - 1)/\zeta^3$, where ζ is the actual distance from the center of the core, $\zeta = (\zeta_1^2 + \zeta_2^2 + \zeta_3^2)^{1/2}$ with $\zeta_1 = \lambda\cos\varphi\sin\theta_1 + r\sin\theta$, $\zeta_2 = \lambda\sin\varphi\times\sin\theta_1$, and $\zeta_3 = \lambda\cos\theta_1 + r\cos\theta$. The mean local field faced by a nucleus at the point $\boldsymbol{r}(\theta,r)$ is then

$$B(\theta,r) = (A/2)\int_0^{\pi}\int_0^{2\pi}[(3\cos^2\theta_1 - 1)\sin\theta_1/\varsigma^3]\,\mathrm{d}\varphi\,\mathrm{d}\theta_1 \quad (5)$$

and $\nu(r,\theta)$ in eq 3 is $\gamma B(\theta,r)$. It can be shown that even relatively slow diffusion both symmetrizes and narrows the signal, according to eq 5. At the same time, however, the diffusion motion of the nucleus in the magnetic field gradient $g(\theta_1,\zeta) = (\partial/\partial\zeta + \partial/\partial\theta_1)B(\theta_1,\zeta)$ causes dephasing $M(\tau) = M_0\exp(-D\gamma^2g^2(\theta_1,\zeta)^2\tau^3/3)$ leading to a diffusion broadening of the signal

$$\Delta w_\mathrm{d}(\theta_1,\varsigma) = D\gamma^2g^2(\theta_1,\zeta)\tau^2/6\pi \quad (6)$$

Analytical expression of $g(\theta_1,\zeta)$ is possible but complex. On this level of approximation, it appears to be permissible to express it in a difference form $g(\theta_1,\zeta) = [B(\theta_1,\zeta) - B(\theta,r)]/(\zeta - r)$. The mean signal broadening $\Delta w_\mathrm{d}(\theta,r)$ at the point (θ,r) is then

$$\Delta w_\mathrm{d}(\theta,r) = (1/24\pi)A^2\int_0^{\pi}\int_0^{2\pi}\{[B(\theta_1,\varsigma) - B(\theta,r)]^2/(\varsigma - r)\}\,\mathrm{d}\varphi\,\mathrm{d}\theta_1 \quad (7)$$

and the signal shape is described again by eq 3, substituting $\nu(r,\theta)$ by $\gamma H(\theta,r)$ and w by $w + \Delta w(\theta,r)$, respectively. The combined effects of diffusion averaging/narrowing (eq 5) and broadening (eq 7) lead to a symmetrized and only slightly narrowed signal if the diffusion coefficient is low, as demonstrated in Figure 3 using the same parameters as in Figure 1 but including diffusion ($D = 10^{-14}$,10^{-13}, or 10^{-12} m^2 s^{-1}). It has to be emphasized that we mean self-diffusion conserving the overall radial distribution of the solute but allowing for lateral exchange of individual molecules. Such situation can occur if the solute forms a diffuse pseudophase around the spherical object (such as the monomer at the micellar core−shell interface) but is not immobilized by adsorption.

Polymerization Kinetics under General Radial Monomer Distribution. Let us denote as $I(r,t)$, $I^*(r,t)$, $M(r,t)$, $P^*(r,t)$, and $P_n(r,t)$ the instant radially dependent concentrations of initiator, initiator radicals, monomer, polymer radicals, and the terminated polymeric n-mer, respectively. In our first approximation, $I(r,t) = I(t)$, i.e., the initiator is evenly distributed and its concentration is affected only by its conversion; also, the polymerization is not diffusion-controlled and the starting monomer concentration $M_0(r,t)$ is given by the radial profile $g(r)$. In such case, the kinetics is described by three coupled differential equations

$$\frac{\mathrm{d}I^*(r,t)}{\mathrm{d}t} = 2k_\mathrm{d}I_0\exp(-k_\mathrm{d}t) - k_\mathrm{i}I^*(r,t)M(r,t) \quad (8a)$$

$$\frac{\mathrm{d}P_1^*}{\mathrm{d}t} = k_\mathrm{i}I^*(r,t)M(r,t) - k_\mathrm{t}P_1^*(r,t)\sum_{i=1}^{\max}P_i^*(r,t) \quad (8b)$$

$$\frac{\mathrm{d}M(r,t)}{\mathrm{d}t} = -[k_\mathrm{i}I^*(r,t) + k_\mathrm{p}P^*(r,t)]M(r,t) \quad (8c)$$

where k_d, k_i, k_p, and k_t are the rate constants of initiator decomposition, initiation, propagation, and termination, respectively.

The situation changes if there is some mass redistribution due to polymerization. For instance, if the polymer starting from the critical chain length n_crit tends to migrate into the interior of the micellar shell, the radius-dependent description is ($n \geq n_\mathrm{crit}$):

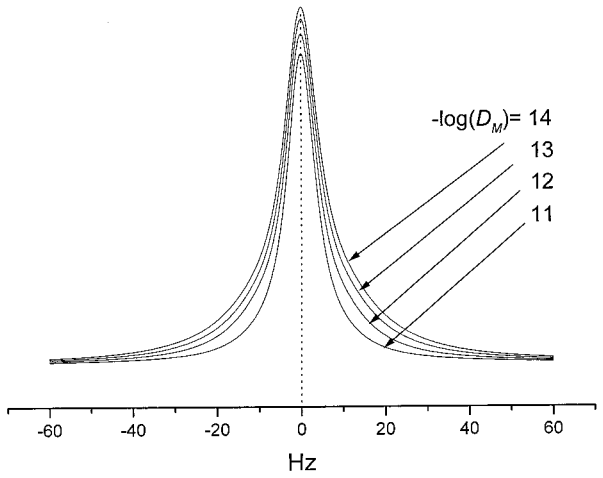

Figure 3. NMR signal shapes simulated for the same conditions as in Figure 1 but with included self-diffusion of the molecules ($D = 10^{-14}$, 10^{-13}, 10^{-12}, 10^{-11} m^2 s^{-1}).

$$\frac{\partial P_n^*}{\partial t} = k_\mathrm{p}P_{n-1}^*M(r,t) + \frac{\partial}{\partial r}\left[D_n(r,t)\left(\frac{\partial}{\partial r} + 2/r\right)\right]P_n^* - k_\mathrm{t}P_n^*\sum_{i=1}^{\max}P_i^* \quad (9a)$$

$$\frac{\partial P_n}{\partial t} = \frac{\partial}{\partial r}\left[D_n(r,t)\left(\frac{\partial}{\partial r} + 2/r\right)\right]P_n + k_t\sum_{i=1}^{n-1}\sum_{j=n-i}^{1}P_i^*P_j^* \quad (9b)$$

where P_x^* is an abbreviation for $P_x^*(r,t)$.

Equations 9a,b as such do not explicitly reflect two features of the system: (i) the polymer concentration at any value of r has an upper bound given by the polymer self-saturation; and (ii) starting with some chain length n_crit, the polymer (or polymer radical) is virtually insoluble in water and its migration into the outer parts of the micellar shell is thus improbable. As an approximate solution of these problems, we can assume that the material transport of the polymer or polymer radical of the length n is driven not by the concentration $P_n(r,t)$ (or $P^*_n(r,t)$) but by its distance from saturation. Given some radial saturation profile $g_n(r)$, the corresponding term of material transport would thus be

$$\frac{\partial P_n(r,t)}{\partial t} = \frac{\partial}{\partial r}\left\{D_n(r,t)\left[\frac{\partial}{\partial r} + (2/r)\right][g_n(r) - P_n(r,t)]\right\} \quad (10)$$

According to eq 10, material flows against the concentration gradient and converges to zero near saturation. Diffusion coefficient $D_n(r,t)$ generally depends on actual polymer concentration; not knowing the actual form of this dependence, we assume it, in first approximation, to be constant. Equations 9a,b then acquire the form

$$\frac{\partial P_n^*}{\partial t} = k_\mathrm{p}P_{n-1}^*M + D_n\left[\frac{\partial^2}{\partial r^2} + \frac{2}{r}\frac{\partial}{\partial r}\right][g_n(r) - P_n^*] - k_\mathrm{t}P_n^*\sum_{i=1}^{\max}P_i^* \quad (11a)$$

$$\frac{\partial P_n^*}{\partial t} = D_n\left[\frac{\partial^2}{\partial r^2} + \frac{2}{r}\frac{\partial}{\partial r}\right][g_n(r) - P_n] + k_t\sum_{i=1}^{n-1}\sum_{j=n-i}^{1} P_i^* P_j^* \quad (11b)$$

At the same time, the initiator molecules are driven out of the inner-shell area by the accumulating polymer. As this process is also controlled by polymer saturation, we can use an analogous diffusion principle driving the initiator concentration to zero near the saturation of the area by polymer. The initiator concentration is then described by the approximate relation

$$\frac{\partial I(r,t)}{\partial t} = -k_d I(r,t) - \{D_I/[g_P(r) - P_r(r,t)]\}\left[\frac{\partial^2}{\partial r^2} + \frac{2}{r}\frac{\partial}{\partial r}\right] \times I(r,t) \quad (12)$$

We need not care for the material transport of the initiator radicals, their concentration being very low, but we have to rewrite eq 8a into the form

$$\frac{dI^*(r,t)}{dt} = 2k_d I(r,t) - k_i I^*(r,t) M(r,t) \quad (13)$$

Also, the radial concentration of monomer $M(r,t)$ should not be much affected by polymer accumulation. The material transport of monomer can be important, however. Hence we have to rewrite eq 8c, too:

$$\frac{\partial M(r,t)}{\partial t} = -[k_i I^*(r,t) + k_p P^*(r,t)]M(r,t) + \frac{\partial}{\partial r}\left[D_M\left(\frac{\partial}{\partial r} + \frac{2}{r}\right)\right]M(r,t) \quad (14)$$

The diffusion coefficient of the monomer D_M can depend on the polymer concentration P due to changing viscosity of the medium.

Equations 11−14 form a model of the polymer kinetics. For simulations, we have to restrict it further, namely by assuming that the polymer growth is much faster than diffusion. This permits us to drop the subscript n in eqs 11a,b; rewriting them again, we get

$$\frac{\partial P^*}{\partial t} = k_p I^* M + D_P\left[\frac{\partial^2}{\partial r^2} + \frac{2}{r}\frac{\partial}{\partial r}\right][g_P(r) - P]P^* - k_t P^{*2} \quad (15a)$$

In eqs 17a,b, the symbols P and P^* stand for $P(r,t)$ and

$$\frac{\partial P}{\partial t} = k_p P^* M + D_P\left[\frac{\partial^2}{\partial r^2} + \frac{2}{r}\frac{\partial}{\partial r}\right][g_P(r) - P] + k_t P^{*2} \quad (15b)$$

$P^*(r,t)$, respectively, i.e., the radius- and time-dependent concentrations expressed in moles of the monomer units per liter, irrespective of the polymer length. Equations 12−15, rewritten in a difference form, were used for computer simulations. The algorithm used a fixed integration step in r dimension and an adaptive one in t. As the starting monomer distribution function $g(r)$, we used the Gaussian distribution with $b = 1.65$ fitting well the experimental results (see below). In deriving the polymer saturation profile, we consider the free volume in the micellar shell interior. In the radius interval $\langle R + n\lambda_m, R + (n+1)\lambda_m\rangle$, the volume available for the polymer is $V_n = (4\pi/3)\{[R + (n+1)\lambda_M]^3 - [R + n\lambda_m]^3\} - NV_m$, where λ_m and V_m are the statistical equivalent length and excluded volume of PMA monomer unit, respectively, and N is the number of PMA chains in one micelle. Applying a quasi-continuum approximation substituting V_m by an equivalent cylinder, one can calculate an outer radius r_b of the densely packed PMMA layer at full MMA conversion. For example, in the experimental case with the micellar concentration $c_{mic} = 1.67$ g/L, $R = 10.2$ nm, and $N = 166$, $r_b = 1.606R$ for $M_0 = 0.002$ vol/vol, the van der Waals volume of the PMA unit having been calculated by ab initio SCF calculation for a pentamer chain. We apply now in a purely phenomenological way a modified Gompertz population function

$$g_P(r) = C_P\{1 - \exp[-\exp(-\kappa(r - r_b))]\} \quad (16)$$

for the polymer saturation profile, where C_p is the polymer concentration in bulk, $C_P = 1000 s_P/m$ with s_P the specific weight in g/mL and m the molecular weight of the monomer unit; κ characterizes the sharpness of the PMMA−D_2O interface (for $\kappa > 10$, eq 16 is almost a step function, $\kappa < 2$ gives a fairly diffusive profile allowing thus the polymer to be partly distributed along the PMA chains). When comparing the simulated conversion curves with the experimental ones, we came to the conclusion that termination of the polymer growth must be markedly suppressed in the interface at higher conversions, in a kind of gel effect. Therefore, we included the dependence $k_t = k_t(P)$ into the model, using a purely phenomenological function $k_t(P) = k_{t0}\exp(-xP)$, x being varied from 0.5 to 3; the optimum value appeared to be around 2.3.

The mathematical model described by eqs 12−5 is based on the assumption that all the reactants and products remain in the area of the micellar shell or the core−shell interface. For the monomer, this is not exactly true. It can, in particular at higher temperature, diffuse into the core and be shielded there by the core polymer from the attack of initiator or polymer radicals (see below). We have thus to include the core area ($r \in \langle 0, R\rangle$) into the model, the appropriate equation for the monomer being

$$\frac{\partial M(r,t)}{\partial t} = -\frac{\partial}{\partial r}\left[D_M(r,t)\left(\frac{\partial}{\partial r} + \frac{2}{r}\right)\right]M(r,t) \quad (17)$$

where the diffusion coefficient of the monomer $D_M(r,t)$ generally increases with increasing monomer concentration $M(r,t)$. In simulation, this effect should be included; in measurement, however, the signals of the monomer residing in the core and at the interface can be distinguished (see below). The overall monomer concentration observed by NMR is then given by the formula

$$M(t) = \psi 4\pi \int_R^{r_{max}} r^2 M(r,t)\, dr \quad (18)$$

where ψ is an appropriate normalization constant.

We present simulations of the conversion curves together with experimental data below. Here, we give an example of the corresponding development of the radial concentration profile of the polymer $P(r,t)$ obtained from the model fitting the experimental conversion curve for $M(0) = 0.02$ mol/L and $T = 330$ K. In Figure 4a,b, radial profiles at different reaction times are compared, the model skipping (Figure 4a) and including (Figure 4b, this case fitting well the experimental conversion curve) the diffusion of the polymer

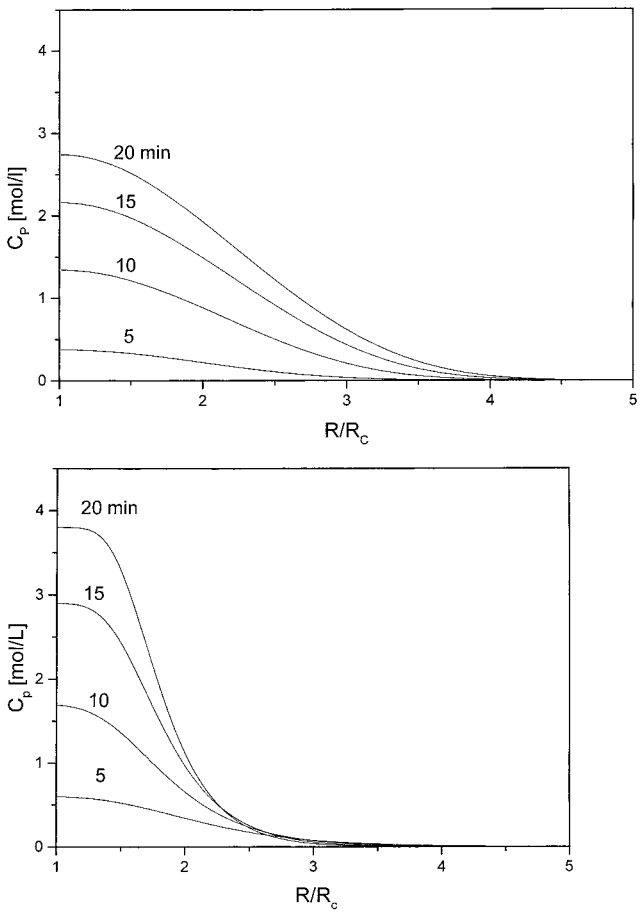

Figure 4. Radial concentration profiles of the polymer simulated for different polymerization times without (a, top) and with (b, bottom) the diffusion of the polymer to the core−shell interface (k_p = 143 mol L s^{-1}, $k_d = 3.16 \times 10^{-6}$ L s^{-1}, $k_t = 1.2 \times 10^5$ mol L s^{-1}, $D_P = 2 \times 10^{-12}$ m^2 s^{-1}, κ = 6.0, $r_b = 1.5R$).

to the core−shell interface. As seen, a rather densely packed peel of the polymer is formed at the interface in the second case. This result agrees with our NMR results and can be verified by SANS.

Experimental Part

A solution of polystyrene-*block*-poly(methacrylic acid) micelles (1.67 g/L) in 0.1 M Borax in D_2O was prepared by the procedure described earlier.[18] Nitrogen was bubbled through the solution for 5 min, and then an appropriate amount (mostly 2 or 4 g/L) of MMA (Aldrich reagent grade, purified by distillation), 50 mL/L of 10% w/w solution of sodium peroxysulfate (Aldrich reagent grade, recrystallized from water solution) in D_2O was added. In the case of polymerizations at normal temperature, 50 mL/L of 10% w/w solution of sodium disulfite (Aldrich reagent grade, recrystallized) was added as a redox agent before the peroxysulfate. The mixture was transferred into a NMR tube flushed with nitrogen. The tube was then sealed and put into the probe head of a Bruker Avance DPX 300 NMR spectrometer, thermostated at the given temperature, and preshimmed with a similar probe. Serial ^{1}H NMR spectra were measured taking 16 scans of 16 kpoints with a repetition time 7 s. Exponential weighting with lb = 1.0 Hz was used for quantitative evaluation before Fourier transform. For signal shape analysis, no weighting was used.

Results and Discussion

The micellar solution used was based on a polystyrene-*block*-poly(acrylic acid) copolymer with M_w = 42 400 and 58% w/w of polystyrene. Its medium was 0.1 M Borax solution in D_2O concentration 1.67 g/L. According to SANS measurements,[15] the micelles exhibited a monodisperse, rather narrow distribution with the core radius R = 102 Å and the average number of block copolymer macromolecules N = 166.

Distribution of Methyl Methacrylate in the Micellar System. Figure 5 compares ^{1}H NMR spectra of a 0.02 M solution of MMA in (a) 0.1 M Borax in D_2O and (b) 0.167% w/w solution of the polystyrene-*block*-poly(methacrylic acid) micelles in 0.1 M Borax solution in D_2O at 296 K. For illustrative reasons, the system corresponding to spectrum b was measured after a two-week storage due to which a part of MMA diffused into the outer layer of the micellar core. Because of the quasi-glassy state of the poly(styrene) core and lowered mobility of the poly(methacrylic acid) shell, the signals of the micelles are broadened beyond detection and are not visibly present in spectrum b; except the signals of impurities (mostly residual dioxane in the micellar solution), only signals of MMA are present. As easily seen, the signals of D_2O-dissolved MMA (vinyl protons 6.1 and 5.7, O−CH_3 3.75 and α-CH_3 1.91 ppm, respectively) remain at the same positions in the micellar solution but are distinctly broadened and, at closer inspection, slightly asymmetric. In contrast, the second set of MMA signals (vinyl protons 5.64 and 5.35, O−CH_3 3.31 and α-CH_3 1.84 ppm) are shifted and distinctly narrower. It can be shown that this second set corresponds to MMA absorbed into the micellar core: (i) by prolonged heating of the system at 330 K, the intensity of the first set is gradually transferred into the second one; (ii) at higher MMA concentrations and after full transfer of the respective signal intensities, first signs of the polystyrene signals appear; (iii) after equilibrium swelling of the system with chlorobenzene, the intensity of the former set increases again but the signals are slightly upfield-shifted, indicating thus slow exchange between the core and D_2O.

In comparison with all micellar systems studied by us so far, two important differences can be observed: (i) there is very slow exchange between the D_2O- and core-dissolved solute so that separate sets of its signals can be observed; and (ii) the signals of the D_2O-dissolved solute are distinctly broader ($\Delta\nu_{1/2}$ = 9.66 compared with original 2.71 Hz at 6.1 ppm and 3.45 Hz at 5.64 ppm) and slightly asymmetric. As explained in Theory, the plausible explanation of (ii) is an inhomogeneity of a secondary magnetic field induced around the spherical core due to its different magnetic susceptibility. The signals of the solute placed inside the core are not inhomogeneously broadened. However, as the solute is swollen into a rigid poly(styrene), homogeneous signal broadening could be expected. The only plausible explanation of the actual signal width is a high MMA/polystyrene ratio, i.e., high swelling of polystyrene by the monomer. Given the relative intensity of the corresponding MMA signal, most of the solute absorbed by the core must remain at the outer rim of the core. This should be due to a very steep concentration dependence of the diffusion coefficient of the monomer in the core leading to a narrow penetration frontier.[9]

Returning now to the shape of the monomer signals, Figure 6 gives an example of a smoothed-out signal of MMA (0.02 mol/L) at 6.1 ppm with the best simulations using the theoretical model without (curve 2) and with (curve 3) respect to the self-diffusion of the monomer. Both simulations assume the maximum induced broad-

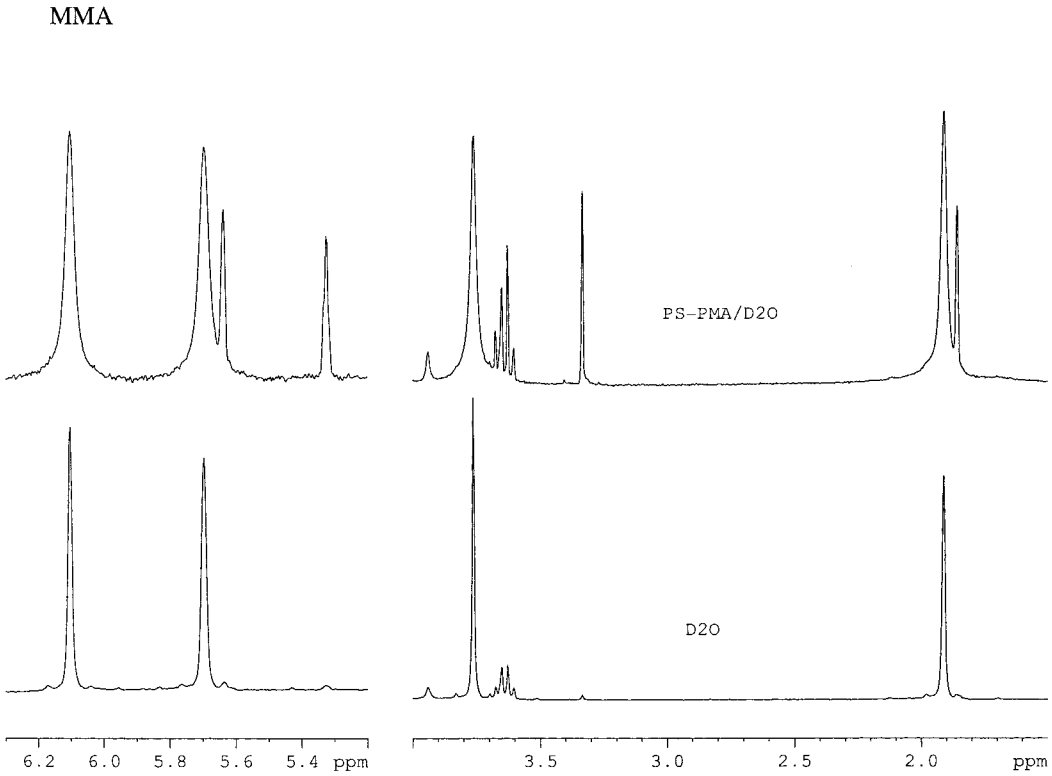

Figure 5. NMR spectra of methyl methacrylate (0.0188 mol/L) in (a, top) 0.1 M Borax in D_2O and (b, bottom) micellar solution of PS-PMA (1.67 g/L) in 0.1 M Borax solution in D_2O (296 K).

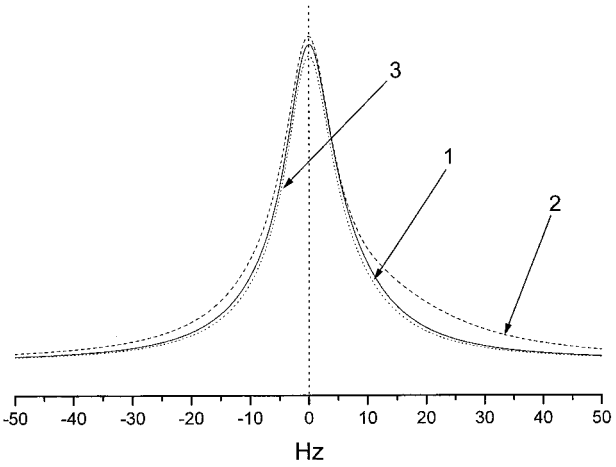

Figure 6. Smoothed-out experimental signal of the *cis*-vinyl proton of MMA in the micellar solution (1) with the simulated signal shapes with disregarded (2) and included (3) MMA self-diffusion ($D_M = 6.3 \times 10^{-12}$ m^2 s^{-1}, maximum broadening 55 Hz, Gaussian radial distribution of MMA with $b = 1.65R$).

ening of 55 Hz and the Gaussian radial distribution of the maximum at the radius of the core R and $b = 1.65R$. In the case of the successful simulation (curve 3), a self-diffusion coefficient $D_M = 6.3 \times 10^{-12}$ m^2 s^{-1} was included with the restriction that diffusion conserves the radial distribution. When increasing the monomer concentration to 0.04 mol/L, the simulated radial distribution broadens to $b = 1.93R$. At 330 K (before substantial absorption of the monomer by the core), the monomer distribution width at 0.02 and 0.04 mol/L somewhat increases to $1.78R$ and $2.17R$, respectively, and the best value of D_M is about 0.8×10^{-10} m^2 s^{-1}.

Both the low values of D_M and the restriction to self-diffusion imply that the monomer forms a dynamic pseudophase in the interior of the micellar shell partly stabilized by positive interactions with the core−shell interface and with the locally hydrophobized PMA chains. It should be noted that the shape of the D_2O-dissolved monomer signals does not change with time except for slight broadening under conditions of slow core swelling which increases the core radius; i.e., the effect is in accord with the theory. Thus, the accumulation of the monomer near the core−shell interface must be accomplished in less than 2 min whereas substantial penetration into the core takes hours (330 K) or days (295 K).

Polymerization Course and Kinetics. During polymerization, the intensity of the MMA signals gradually decreases whereas no signals of the PMMA appear. This indicates that the polymer molecules are formed in an immobilized state (or they reach such state rapidly), their signals being broadened beyond detection mostly by static dipolar interactions. We suggest this effect to be an indication, if not proof, of the polymer diffusion to the core−shell interface already proposed in Theory.

The intensity change of the monomer signals gives us the possibility to measure its conversion, i.e., polymer kinetics. Figure 7 shows such conversion curves for a redox-initiated polymerization at 298 K. Figure 8 contains analogous curves for a peroxysulfate-initiated polymerization at 330 K. In both cases, the course of polymerization is another indirect proof of the monomer accumulation in a relatively small area of the micelle, i.e., with a high local concentration: in the absence of micelles but otherwise the same system, i.e., in a normal solution of MMA, the polymerization takes several hours to reach a substantial conversion. In the simulations of the polymerization course using the mathematical model outlined in Theory, we used published[19] values of k_p ($5.13 \times 10^6 \exp(-2.64 \times 10^4/RT)$) and k_d ($1.36 \times 10^3 \exp(-1.19 \times 10^4/RT)$) but we were unable to find

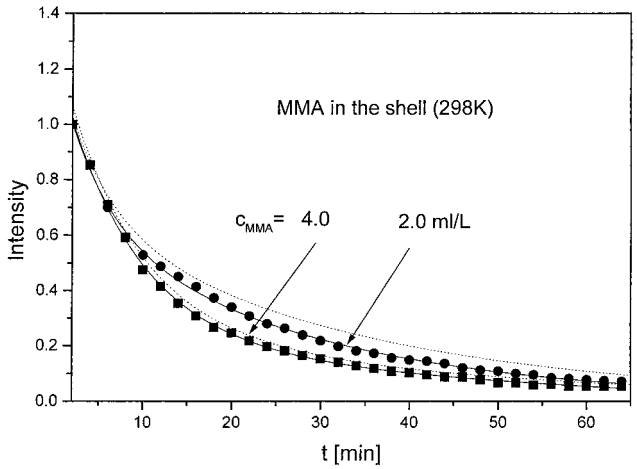

Figure 7. Experimental and simulated conversion curves of MMA polymerization for the given concentrations of the monomer at 298 K (dotted curves: best simulations without progressively damped termination; for the constants used, see the text).

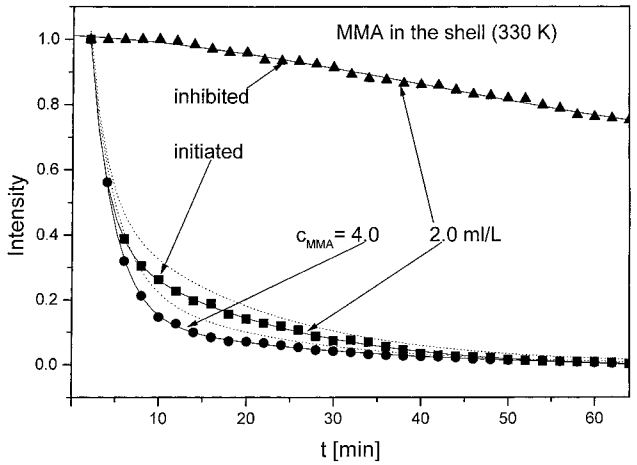

Figure 8. Time dependence of the monomer concentration in the micellar shell under polymerization initiation or inhibition at 330 K (all starting concentrations normalized to unity).

even a passable agreement with the experimental data using the published termination constants k_t. We actually had to use the starting values at least 2 orders of magnitude lower (i.e., 8×10^4 and 12×10^4 mol L s^{-1} at 298 and 330 K, respectively), the best simulations being shown by the dashed curves in Figures 7 and 8. A better agreement with experimental data was achieved when using a conversion-dependent termination constant as outlined in Theory, with the coefficient $x = 2.3$. This effect is not quite clear; a most plausible explanation appears to be a kind of gel effect in a relatively dense and immobilized polymer layer. Therefore, the model including the diffusion of the polymer and radicals into the interface area was applied, using $D_P = 2 \times 10^{-12}$ m^2 s^{-1}.

At 330 K, another complication of the process emerges. As shown in Figures 8 and 9, part of the monomer escapes from the polymerization area into the core. The process competes with polymerization and, consequently, is slower in the polymerizing system than in the inhibited one (Figure 9). There is an interesting difference in this respect between the two starting monomer concentrations: whereas the amount of the core-bound monomer converges at a higher concentration (0.04 mol/L) to an almost constant value, at a lower

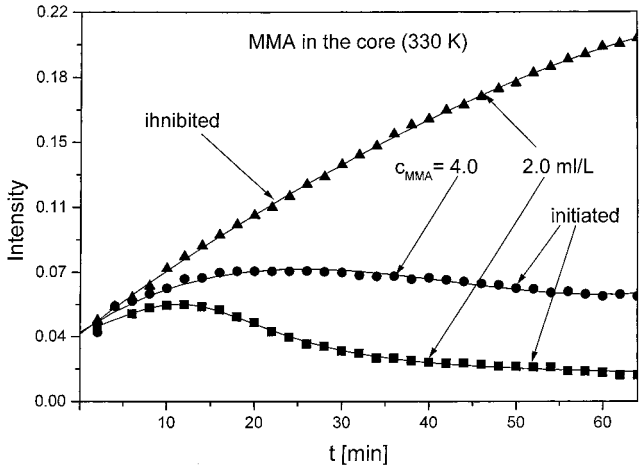

Figure 9. Time dependence of the monomer concentration in the micellar core under polymerization initiation or inhibition at 330 K (intensity scale the same as in Figure 8).

one (0.02 mol/L), it passes through a maximum and decreases again to a quite small value. There are two possible explanations of this effect at the lower monomer concentration: (i) the equilibrium between the core- and interface-bound monomer shifts back at higher conversion of the monomer; (ii) the core-bound monomer is more approachable for the initiator or polymer radicals, i.e., less shielded from them by the polymer accumulating at the core−shell interface. Both explanations imply that the core-bound monomer is mostly placed at the surface layer of the core, which is in agreement with the above-discussed narrowness of its signal. In the case (ii), the core-bound monomer takes part in the polymerization process. This possibility can be neither confirmed nor excluded by NMR.

From the practical point of view, i.e., the possibility to prepare multilayered micelles by a simple polymerization technique, the MMA polymerization in the outer layers of the core is not a serious flaw: it only makes the interface between the two polymers somewhat fuzzy. As shown, this can be avoided by lowering the polymerization temperature using a redox initiator system.

Conclusions

According to our NMR signal shape analysis based on the presented mathematical model, polystyrene-*block*-poly(methacrylic acid) micelles at their concentration 1.67 g/L in a 0.1 M Borax solution in D_2O take up into their shells up to 2.25 their weight of dissolved methyl methacrylate, distributing it in an approximately Gaussian distribution near their core−shell interface. The absorbed monomer can be polymerized using a water-soluble initiator such as ammonium or sodium peroxysulfate (at 60 °C) or better its mixture with a reducing agent such as sodium or potassium disulfite (at ambient temperature). If the polymerization follows shortly after monomer addition and proceeds at low temperature, the monomer does not swell into the micellar core and the polymer forms a densely packed layer at the core−shell interface. A novel technique of preparing polymer micelles with multilayered cores has thus been demonstrated. It has to be admitted, however, that this technique could fail when using micelles with entirely different structure. Very probably, its success implies the satisfaction of two requirements: (i) before initiation, the monomer has to be distributed near the core−shell interface and (ii) it should not penetrate the

core with a rate comparable to polymerization. The point (i) is probably satisfied if the micellar shell tends to form hydrophobic domains near the core−shell interface, which is the case with poly(methacrylic acid) but much less so with poly(acrylic acid) or even its alkali salt. The point (ii) implies rather hard cores formed by polymers in a glassy state; the uptake of the solute by a semifluid core[9] should prevent polymerization at the interface. However, the scope of experiments presented here prevents final conclusions in this direction. Further research is thus intended.

Acknowledgment. The authors thank the Grant Agency of the Academy of Sciences of the Czech Republic and the Grant Agency of the Czech Republic for their financial support given under the grants K2050602/12 and 203/97/249.

References and Notes

(1) Tuzar, Z.; Webber, S. E.; Ramireddy, C.; Munk, P. *Polym. Prepr.* (*Am. Chem. Soc., Div. Polym. Chem.*) **1991**, *32* (1), 525.
(2) Hurter, P. N.; Hatton, T. A. *Langmuir* **1992**, *8*, 1291.
(3) Kiserow, D.; Procházka, K.; Ramireddy, C.; Tuzar, Z.; Munk, P.; Webber, S. E. *Macromolecules* **1992**, *25*, 4613.
(4) Zhang, L.; Eisenberg, A. *Science* **1995**, *268*, 1728.
(5) Chu, B. *Langmuir* **1995**, *11*, 414.
(6) Moffit, M.; Zhang, L.; Khougaz, K.; Eisenberg, A. In *Solvents and Selforganization of Polymers*; Webber, S. E., Munk, P., Tuzar, Z., Eds.; Kluver Academic Publishers: Dordrecht, 1996; p 53.
(7) Nagarjan, R.; Barry, M.; Ruckenstein, E. *Langmuir* **1986**, *2*, 210.
(8) Tian, M.; Arca, E.; Tuzar, Z.; Webber, S. E.; Munk, P. *J. Polym. Sci. B, Polym. Phys.* **1995**, *33*, 1713.
(9) Kříž, J.; Masař, B.; Doskočilová, D. *Macromolecules* **1997**, *30*, 4391.
(10) Kříž, J.; Masař, B.; Pleštil, J.; Tuzar, Z.; Pospíšil, H.; Doskočilová, D. *Macromolecules* **1998**, *31*, 41.
(11) Procházka, K.; Martin, T. J.; Webber, S. E.; Munk, P. *Macromolecules* **1996**, *29*, 6526.
(12) Talingting, M. R.; Munk, P.; Webber, S. E.; Tuzar, Z. *Macromolecules* **1999**, *32*, 1593.
(13) Kříž, J.; Pleštil, J.; Tuzar, Z.; Pospíšil, H.; Brus, J.; Jakeš, J.; Masař, B.; Vlček, P.; Doskočilová, D. *Macromolecules* **1999**, *32*, 397.
(14) Munk, P.; Arca, E.; Cao, T.; Webber, S. E. Paper presented at the National ACS Meeting, San Diego, CA,1994.
(15) Pleštil, J.; Pospíšil, H.; Kadlec, P.; Tuzar, Z.; Kříž, J.; Gordeliy, V. I. *Macromol. Chem. Phys.*, submitted for publication.
(16) Stratton, J. A. *Electromagnetic Theory*; McGraw-Hill: New York, 1941.
(17) Doskočilová, D.; Tao, D. D.; Schneider, B. *Czech. J. Phys. B* **1975**, *25*, 202.
(18) Kiserow, D.; Procházka, K.; Ramireddy, C.; Tuzar, Z.; Munk, P.; Webber, S. E. *Macromolecules* **1992**, *25*, 461.
(19) Kamachi, K.; Yamada, B. In *Polymer Handbook*, 4th ed.; Brandrup, J. E., Immergut, H., Grulke, E. A., Eds.; John Wiley and Sons: New York, 1999.

MA991368N